Site-dependent charge transfer at the Pt(111)-ZnPc interface and the effect of iodine

Sareh Ahmadi,[1,a)] Björn Agnarsson,[2] Ieva Bidermane,[3] Bastian M. Wojek,[1] Quentin Noël,[1] Chenghua Sun,[4] and Mats Göthelid[1,a)]

[1]*KTH Royal Institute of Technology, ICT MNF Materials Physics, Electrum 229, 16440 Kista, Sweden*
[2]*Department of Applied Physics, Biological Physics, Chalmers University of Technology, Fysikgränd 3, 412 96 Göteborg, Sweden*
[3]*Department of Physics and Astronomy, Uppsala University, Box 516, 75120 Uppsala, Sweden*
[4]*Australian Institute for Bioengineering and Nanotechnology, The University of Queensland, Brisbane, St Lucia QLD 4072, Australia*

The electronic structure of ZnPc, from sub-monolayers to thick films, on bare and iodated Pt(111) is studied by means of X-ray photoelectron spectroscopy, X-ray absorption spectroscopy, and scanning tunneling microscopy. Our results suggest that at low coverage ZnPc lies almost parallel to the Pt(111) substrate, in a non-planar configuration induced by Zn-Pt attraction, leading to an inhomogeneous charge distribution within the molecule and an inhomogeneous charge transfer to the molecule. ZnPc does not form a complete monolayer on the Pt surface, due to a surface-mediated intermolecular repulsion. At higher coverage ZnPc adopts a tilted geometry, due to a reduced molecule-substrate interaction. Our photoemission results illustrate that ZnPc is practically decoupled from Pt, already from the second layer. Pre-deposition of iodine on Pt hinders the Zn-Pt attraction, leading to a non-distorted first layer ZnPc in contact with Pt(111)-I($\sqrt{3}\times\sqrt{3}$) or Pt(111)-I($\sqrt{7}\times\sqrt{7}$), and a more homogeneous charge distribution and charge transfer at the interface. On increased ZnPc thickness iodine is dissolved in the organic film where it acts as an electron acceptor dopant. © *2014 AIP Publishing LLC*. [http://dx.doi.org/10.1063/1.4870762]

I. INTRODUCTION

During recent years, studies on the growth of phthalocyanine (Pc) films on different surfaces, especially metallic substrates have become a major field for the surface science and organic electronic communities. These molecules can create self-assembled layers, which make the thin-film processing very convenient.[1–8] Phthalocyanines are synthetic macrocyclic compounds, constructed of four lobes; each lobe is composed of one pyrrole and one benzene group. Metal-free phthalocyanine (H_2Pc) is noted as $H_2C_{32}N_8H_{16}$. The flexibility of this molecule provides an opportunity to replace the two central H atoms with a metallic atom (*M*Pc) (a metal-oxygen or metal-halogen can also be inserted into the Pc center). This property has made these molecules very attractive for research, since electronic, optical, physical and magnetic properties of Pcs can be tuned by changing the metallic center.[7–11] In particular, research on transition-metal phthalocyanines has received lots of attention, owing to the significant effect of the d-orbitals on molecular properties.[12–23] These intrinsically semiconducting molecules show very high thermal (stable up to $500\,°C$) and chemical stability in addition to their electronic, optical, and magnetic properties. These characteristics make *M*Pc a promising candidate to be used in organic solar cells,[24–26] organic light-emitting diodes (OLEDs),[27,28] and organic field-effect transistors (OFETs).[25,29] The function of these devices is influenced by another essential factor: interac-

tion and charge transfer at the interface between *M*Pc and substrate. Numerous studies, applying several experimental and theoretical methods, have been carried out to investigate the interfacial interaction and charge transfer, as well as the effect of these interactions on the device functionality. Interaction at the interface between *M*Pc and substrate determines the layer growth mode, molecular configuration, charge transfer, magnetic and optical properties of the molecular layer, which could effectively modify the organic device function. This has encouraged many groups to investigate the effect of substrate-adsorbate interaction on the properties of the molecular layer and consequently the potential devices which would have organic components of similar nature.[5, 12, 18, 30–42]

Manipulation of the *M*Pc-substrate interaction is possible by either decorating the molecules (adding external atoms or molecules to the center or the periphery of Pcs),[43–45] by modifying the substrate by inserting intermediate layers,[46,47] or by adding layers on top of *M*Pc.[48–52] For instance, upon adsorption of pyridine on an ordered layer of FePc on Au(111), pyridine molecules coordinate to the iron. This coordination leads to a strong ligand field which modifies the magnetic and electronic properties of the iron atom.[50] In another study, Gerlach *et al.*[45] showed that by fluorination of CuPc adsorbed on Cu(111) and Ag(111), the molecular distortion and interfacial interactions are modified. Due to the interaction with the substrate, CuPc is adsorbed non-planar on these substrates, yet parallel to the sample surface in both cases. They reported that fluorination resulted in a reduction of the molecule-substrate attraction and consequently a more

"planar" molecular configuration, with the molecular layer further away from the substrate. Bending of MPc molecules on different substrates has been reported, which generally comes together with an inhomogeneous charge transfer at the interface between molecule and substrate.[7,11,12,19,53]

In this article, we have studied the electronic structure of ZnPc on Pt(111) and on two iodine induced surface structures, from sub-monolayer to thick films.

II. EXPERIMENTAL DETAILS

The spectroscopy experiments were done at beamline D1011, at MAX-lab, Swedish national synchrotron radiation laboratory. D1011 is a bending-magnet beamline which offers photons in the energy range 40 eV to 1500 eV selected by a modified SX-700 plane grating monochromator.[54] The experimental system consists of separate analysis and preparation chambers accessible via a long-travel manipulator.

The photoelectron spectra were measured using a SCIENTA SES200 (upgraded) electron energy analyzer. The binding energy of all photoelectron spectra is calibrated with respect to the Fermi level, measured directly on the Pt sample. These spectra are normalized to the background at the low-binding-energy side of the core-level spectra. The total experimental resolution for core-level spectra are 180 meV ($h\nu = 490$ eV, N1s), 100 meV ($h\nu = 382$ eV, C1s), 20 meV ($h\nu = 125$ eV, Pt4f$_{7/2}$), and 16 meV ($h\nu = 110$ eV, I4d and Zn3d). The photoelectron spectra are obtained at normal emission. Numerical curve fitting is done using Donjiac-Sunjic line profiles, which includes a Lorentzian broadening (W_L) from the finite core-hole life time, a Gaussian broadening (W_G) from limited experimental resolution and sample inhomogeneities and an asymmetry (α) on the high binding energy side due to excitation of electrons across the Fermi level.[55]

For Pt4f$_{7/2}$ best fits were obtained with $W_L = 0.32$ eV, $W_G = (0.30$ to $0.40)$ eV, and $\alpha = 0.09$ to 0.12. While these numbers are $W_L = (0.35$ to $0.45)$ eV, $W_G = (0.40$ to $0.55)$ eV, and $\alpha = 0$ to 0.05 for C1s and $W_L = (0.22$ to $0.25)$ eV, $W_G = (0.45$ to $0.65)$ eV, and $\alpha = 0$ to 0.05 for N1s. To fit I4d we use spin-orbit doublets, with branching ratio (BR) = 1.2, spin-orbit split (SO) = 1.71 eV, $W_L = 0.27$ eV, $W_G = (0.28$ to $0.40)$ eV, and $\alpha = 0.05$ to 0.12.

X-ray absorption spectroscopy (XAS) was collected at the nitrogen K-edge in Total Electron Yield (TEY) mode using an MCP detector. The photon energies were calibrated using the kinetic-energy difference in the Pt4f$_{7/2}$ peak measured by first- and second-order light. The absorption spectra were normalized to the spectrum of a clean sample. XAS were taken at three different angles between the surface plane and the electric-field vector; 80°, 40°, and 0°.

The preparation chamber is equipped with an ion sputtering gun, low-energy electron diffraction (LEED) optics, a gas-inlet system, and ports for evaporators. The base pressure in this chamber was lower than 10^{-10} mbar. The Pt(111) single crystal was purchased from Surface Preparation Laboratory, the Netherlands. Before the measurements, the Pt sample was prepared by cycles of Ar sputtering, annealing in O$_2$ atmosphere and subsequently flashing at higher temperature. Ar

sputtering was done at 2×10^{-6} mbar, for 20 min; annealing in oxygen was done at 2×10^{-6} mbar while the sample was heated to 870 K. After annealing, the sample was flashed at 1100 K. A few cleaning cycles were needed to attain a clean and organized surface. The cleanliness of the sample was confirmed by wide-range PES tracing any expected impurities and eventually finding none. The clean sample showed a sharp 1×1 LEED pattern.

Iodine was deposited on the surface from an electrochemical cell. In this cell an AgI pellet is heated to ~370 K. An ionic current flows through the cell (10 μA in this case) and I$_2$ molecules are emitted into the chamber. A 20 min iodine deposition on Pt(111) results in a $(\sqrt{7} \times \sqrt{7})R19.1°$ reconstruction, confirmed by LEED and I4d photoelectron spectra. Heating this saturated iodine layer, at 430 K it transforms into a $(\sqrt{3} \times \sqrt{3})R30°$ structure, also confirmed by LEED and I4d core-level spectra.

The ZnPc layers were prepared by sublimation from a quartz crucible with a diameter of about 5 mm, after degassing for more than 72 h. The monolayers of ZnPc were obtained by deposition on the substrate kept at room temperature. The molecules were purchased from Sigma-Aldrich (98 % dye content; the remaining 2 % consisted mainly of water, which was removed by the long outgassing). The thickness of the ZnPc layer was estimated from the attenuation of the Pt4f$_{7/2}$ signal and the increase of the N1s and C1s signals. At sufficiently large thickness it is reasonable to apply an exponential attenuation model. The coverage 1 ML refers to the number of molecules needed to cover the Pt(111) surface, and 6 ML is 6 times higher surface coverage, without implying any particular growth mode. We also compare with other similar systems measured on the same beamline. The method is not exact and the values we give are therefore approximate.

Scanning tunneling microscopy (STM) experiments were done in a RHK 3500 UHV STM (in a different system from the photoemission experiments) using mechanically cut Pt-Ir tips in constant-current mode. The sample was prepared in a preparation chamber connected to the STM chamber via a gate valve. This chamber is also equipped with LEED optics, an Ar-ion sputter gun and sample heating. The sample was mounted on a Mo sample holder. The sample temperature was measured with chromel-alumel thermocouples, spot-welded on the side of the sample or by a pyrometer.

III. RESULTS AND DISCUSSIONS

A. ZnPc on Pt(111)

In this section the experimental results from ZnPc on Pt(111) are presented. Below, absorption spectra and core-level photoemission spectra from different steps of the ZnPc deposition on Pt are shown and the effect of ZnPc adsorption on the substrate, as well as reactions at the interface and within the molecular layers is discussed. STM images are also presented from ZnPc layers adsorbed on Pt(111).

1. N K-edge XAS

X-ray absorption spectra measured from a monolayer and a thick film (TF) of ZnPc on Pt(111) at 3 different angles are presented in Figure 1. A monolayer (ML) refers to the
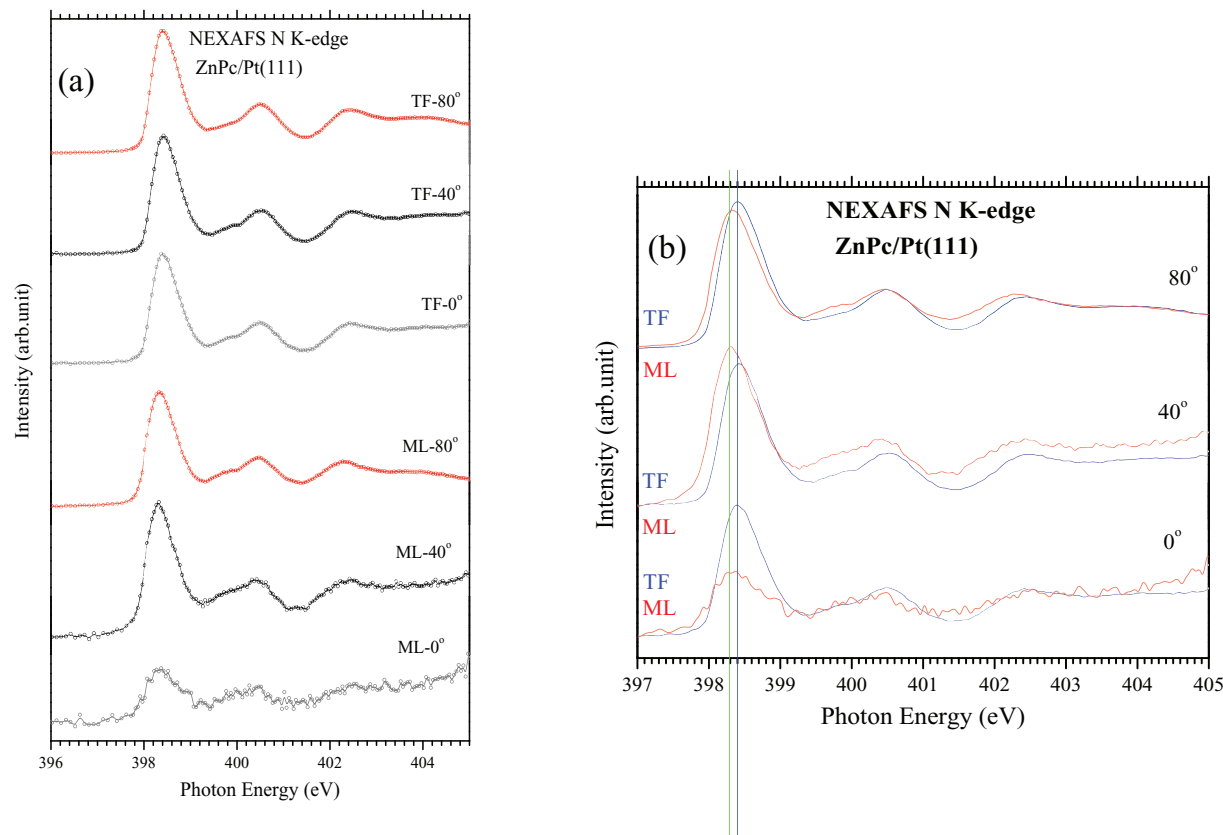
FIG. 1. (a) N K-edge XAS of a monolayer and a thick film of ZnPc on Pt(111), showing that ZnPc molecules are almost flat in the ML regime, but tilted at the TF. (b) Magnification of the π^*-region indicates the participation of nitrogen in the interaction with the Pt substrate at the ML regime.

coverage, in which tightly packed, flat-lying molecules would cover the entire surface;[3] the coverage of TF here is about 10 MLs. The XAS measurement angles are: $\theta = 0°$ (normal incidence), 40° and 80° (grazing incidence), where θ is the angle between the electric-field vector and the surface plane. In the orbital configuration of phthalocyanines π orbitals extend normal to the molecular plane and σ orbitals lie in the molecular plane. In the spectra in Figure 1, excitation into the π^* states are seen as peaks between 397 eV and 403 eV photon energy, while excitation into the σ^* states appears at photon energies above 404 eV.[5] The multiplot demonstrates that molecules are lying almost parallel to Pt(111) in the monolayer, while they are slightly tilted in the thick film.

A closer look at the N K-edge spectra in Figure 1(b) discloses a shoulder-like peak on the lower photon energy side of the first resonance associated to excitation into the LUMO in the ML spectra (marked in Figure 1(b)), especially visible in the spectra measured at $\theta = 40°$ and $\theta = 80°$. Another noticeable change is the variation in the relative intensity of the peaks in each spectrum going from the ML to the TF. A similar behavior was observed for FePc adsorbed on Ag(111) but interestingly not for FePc on Au(100).[15] A splitting of the first resonance is caused by a hybridization of nitrogen orbitals and metal-related states.

2. Pt4f$_{7/2}$ photoemission

In Figure 2, Pt4f$_{7/2}$ photoemission spectra from different sample preparations are presented. The lowermost spectrum
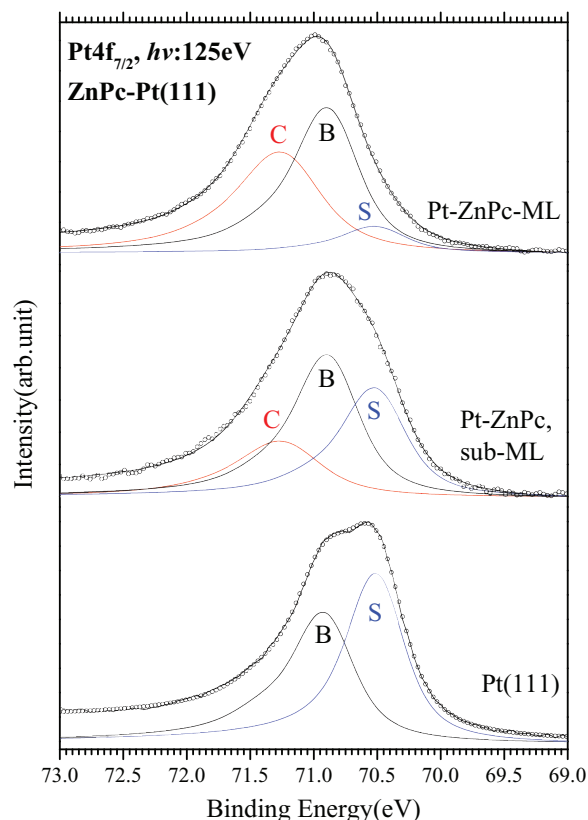

FIG. 2. Pt4f$_{7/2}$ spectra recorded from Pt(111)-ZnPc after different preparations.

is measured from clean Pt(111) and comprises two peaks: the bulk peak at 70.91 eV and the surface peak located at a 0.41 eV lower BE, in good agreement with previous studies.[56–58] Upon adsorption of ZnPc the surface peak loses intensity drastically and is further reduced at higher coverage, unlike the ZnPc/Au(111) system, where even at a high coverage, the surface peak keeps its intensity[5]. Another difference compared to Au(111) is that after adsorption of ZnPc on Pt(111), a new peak (C) appears at higher BE. The appearance of the new chemically shifted peak at E_C following adsorption of organic molecules has been reported previously; e.g., for propene and ethylidine: $\Delta E_C = E_C - E_B = 0.26$ eV, 2-butenal: $\Delta E_C = 0.27$ eV, and CCH_3: $\Delta E_C = 0.36$ eV are observed.[57,59] Adsorption of other molecules such as CO[59] and O_2[56] also resulted in adsorption-induced chemical shifts up to 1 eV, depending on the coverage. Our observation indicates that ZnPc is chemisorbed on Pt(111). The total integrated area under S and C remains roughly at a value which is comparable with the area under the surface peak of the clean surface. Even at the highest coverage, S has 9 % relative intensity, meaning that some surface atoms are untouched by the adsorbate layer. The initial surface peak represents one monolayer of Pt, contributing to 52 % of the total Pt4f$_{7/2}$ intensity. Thus, 9 % represents 0.17 ML of surface atoms.

Kröger *et al.* showed that the D4h symmetry of the molecule is responsible for the vanishing intrinsic electrostatic moment,[2] giving weak intermolecular forces where the favorable adsorption positions are determined mainly by the interaction of molecules with the substrate.[2,34] However, in our case the chemisorption bond will lead to local geometric and/or electronic "deformation" of both substrate and molecule, which as previously shown will create a substrate-mediated intermolecular repulsion.[2]

3. STM

In Figure 3 we present STM images from ZnPc-Pt(111) at sub-monolayer coverage and from a thin film. Figure 3(a) illustrates that ZnPc molecules are lying flat on the surface and are not tightly packed; instead they are sitting far from each other in a scattered manner. A significant observation is that the molecular arrangements are different; in some areas, a few molecules are aligned in one orientation but the arrangement is very local and in connection with the specific region of the substrate. This indicates the determining role of the substrate-molecule interaction and confirms the relatively weaker molecule-molecule interaction mentioned above.[34,60,61] Figures 3(b)–3(d) show images from a multilayer ZnPc-film. Clearly single molecules are resolved in Figure 3(b). ZnPc appears to lie with the molecular plane parallel to the surface, and with a preferred side-to-side alignment to neighboring molecules. However, this ordering does not extend over more than a few molecules. Although the molecular packing is denser, a complete layer is not formed. Instead nanometer-sized holes appear across the surface. Figure 3(c) is a 900×540 Å^2 area, which shows that actually some repeated order exists in a larger view over the surface. Figure 3(d) demonstrate an even larger area over the same re-
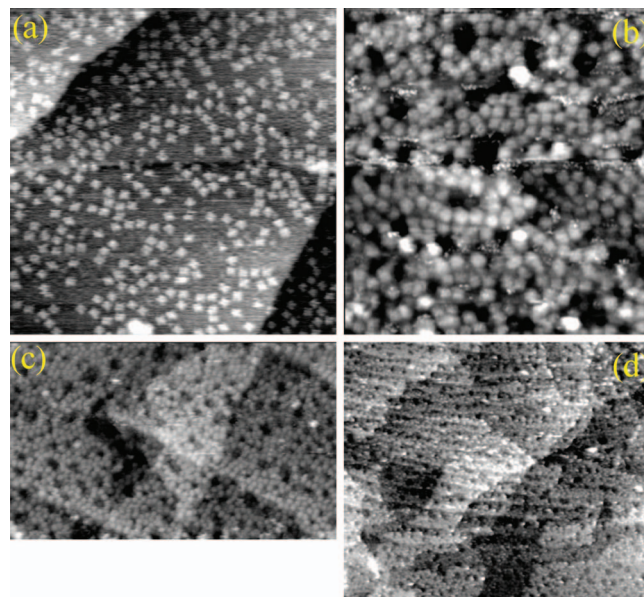

FIG. 3. Room temperature STM images of ZnPc on Pt(111); (a) Sub-ML of ZnPc/Pt(111); 360×360 Å^2, 60 pA, 125 mV, and multilayer of ZnPc/Pt(111): (b) 330×350 Å^2, 68 pA, 9 mV, (c) 900×540 Å^2, 68 pA, 125 mV, and (d) 1800×1600 Å^2, 0.8 nA, 53 mV.

gion (1800×1600 Å^2), confirming the repetitive pattern. The relative area of the holes is on the order of 10 % to 20 %, in good agreement with the Pt4f results, pointing to uncovered Pt in the bottom of the holes (Table I).

A similar porous molecular arrangement was observed for FePc on Au(111) at a so-called higher sub-monolayer coverage, particularly at the elbows of the herringbone structure.[60] Cheng *et al.* explained the origin of this ring-like structure to be the directional attraction between molecules,[60] driven by fitting the benzene group of one molecule to the hollow site of its neighbor. In this position hydrogen atoms of benzene are placed close to nitrogen atoms of the neighboring molecule. Since the nitrogen atom has an unshared pair of electrons and the hydrogen atom possesses a net positive charge, this position is favorable and motivate this ring-like molecular arrangement.[60]

4. Molecular core-level spectroscopy

As mentioned in Subsections III A 1–III A 3, the ZnPc-Pt interaction leads to a reduction of the surface-shifted photoemission peak intensity and the appearance of an extra Pt4f$_{7/2}$ peak at higher binding energy. The binding energy of this chemically shifted peak (C) indicates a charge transfer from Pt to ZnPc. Here, we use the molecular-core-level spectra, measured on a ML and a TF of ZnPc and compare with the

TABLE I. Pt4f curve-fitting results.

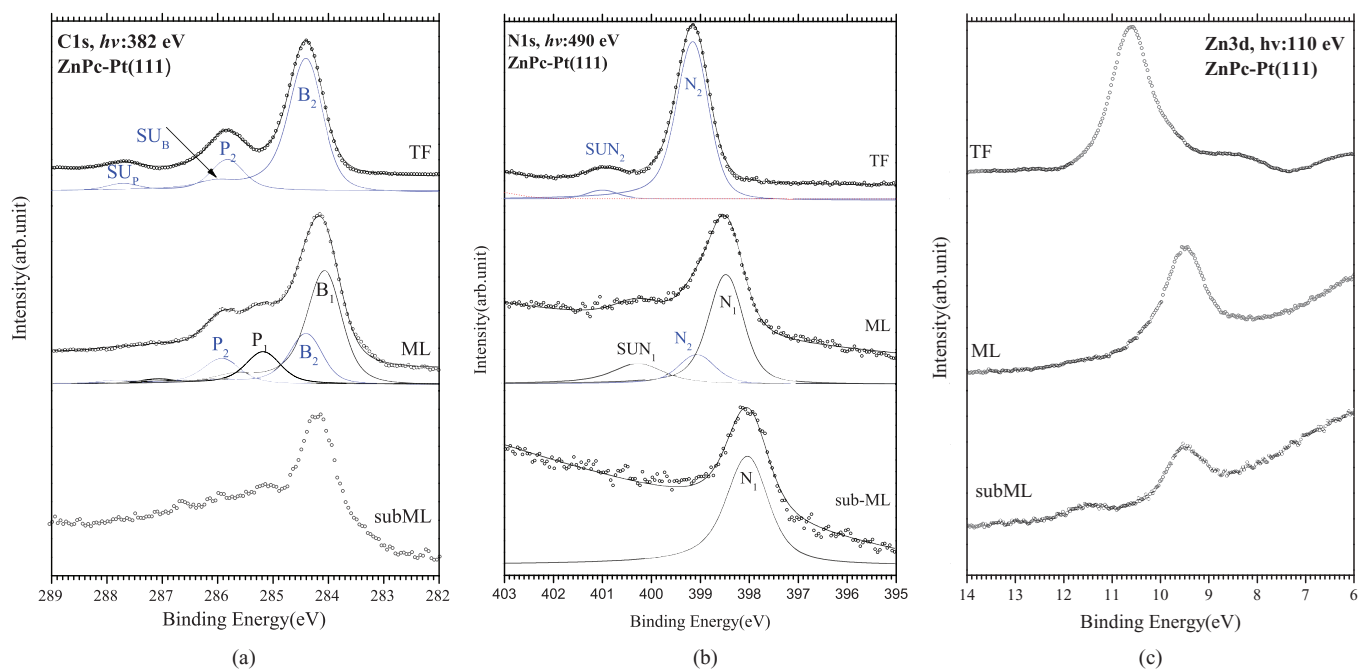|	ΔE_S (eV)	I_S (%)	BE_B (eV)	ΔE_C (eV)	I_C (%)
Pt(111)	0.41	52	70.91	. . .	. . .
Pt-ZnPc-subML	0.37	34	70.91	0.36	22
Pt-ZnPc-ML	0.37	9	70.91	0.36	43

FIG. 4. (a) C1s, (b) N1s, and (c) Zn3d photoemission spectra of ZnPc on Pt(111).

results of ZnPc on Au(111) to investigate the effect of the substrate on the molecular core levels in order to reveal the characteristics of the interaction at the interface.

C1s, N1s and Zn3d photoemission spectra are shown in Figure 4 as a function of molecular layer thickness. In Figure 4(a), C1s spectra are presented. The thick-film spectrum shows a molecular-like C1s spectrum consisting of three peaks; C_B at 284.40 eV (benzene carbon), the second peak contains C_P (pyrrole carbon), and the shake-up of the benzene peak (SU_B); C_P is centered at 285.80 eV, and SU_B and SU_P (shake-up structure of the pyrrole carbon) at 286.03 eV and 287.72 eV, respectively. These peaks are located at the same BE as for the thick film deposited on Au(111).[5]

It is clear that C1s spectra are not molecular-like at low coverage; ZnPc is disturbed by the interaction with Pt. This is not the case when adsorbed on Au surfaces,[5,11,14,19,36,62–65] which are not as reactive as Pt. Yet, on Ag, Cu, and TiO_2 surfaces, C1s spectra are also modified at sub-monolayer thicknesses.[12,53,66] Our curve fitting shows that at ML C1s needs components representing carbon at the interface and carbon in the second layer. There are two C_B (benzene carbon) peaks and two C_P (pyrrole carbon) peaks: interface benzene (B_1) at 284.08 eV and second-layer benzene (B_2), at 284.41 eV. Interface pyrrole (P_1) is at 285.17 eV and second layer pyrrole (P_2) at 285.92 eV. Thus, C_P shifts more than C_B, i.e., pyrrole carbon are more affected by the interfacial interaction than benzene carbon. This site-specific coverage-dependent shifts have been observed before for MgPc on polycrystalline gold, where by increasing the thickness from 0.5 nm to 9 nm, C_B shifted 0.4 eV to higher BE, while C_P shifted 0.6 eV in the same direction.[11] Also in ZnPc/TiO$_2$, C_P shifted 1.5 eV to higher BE in a thick film with respect to a ML, but C_B shifted only 0.8 eV.[12] The C_B peak of the ZnPc

ML is centered at 284.08 eV which is at 0.47 eV higher BE than for a ZnPc ML adsorbed on Au(111) (this is 0.18 eV for C_P).[5] This indicates a lower electron density around the carbon atoms at the interface between ZnPc and Pt(111) than Au(111). There is also a shift to higher BE going from a ML to a TF (0.32 eV for C_B and 0.75 eV for C_P). Generally, this shift is explained as weaker core-hole screening through the substrate at thick films with respect to low-coverage films. This shift also depends on the charge transfer at the interface, i.e., in systems where molecules receive electrons from the substrate, by increasing the coverage the molecules are further from the substrate, the core-level binding energies increase in the thick film.[2] Telling these two sources of a BE shift apart is not straightforward and requires more data analysis; this will be discussed in more detail later in this section. Another noticeable observation is that the binding energies of B_2 and P_2 are the same as C_B and C_P at the thick film, indicating that the molecules are practically decoupled from the substrate already at the second layer (at least the carbon rings). Previously it was claimed that CuPc on Ag(111) was decoupled from the substrate from the third layer (measured at 80 K).[2]

N1s spectra of ZnPc on Pt(111) are shown in Figure 4(b). The thick-film spectrum is a single peak located at 399.16 eV which represents two different groups of nitrogen atoms in the Pc molecule; the separation of these two peaks is too small to be resolved in the spectrum.[67] The shake-up structure is located at 1.82 eV higher BE, the same as observed for ZnPc/TiO$_2$[12] and ZnPc/Au(111).[5] The first two spectra at the bottom are from a sub-ML and ML film and their main peaks are broader than in the thick-film spectrum. The curve-fitting results show that in the ML region, two peaks (with the same line profile as in the TF spectrum) are present: N_1 at lower BE and N_2 at higher BE. Since it seems that in the TF, only

the higher BE peak is present, we ascribe N_1 to the nitrogen atoms directly in contact with the Pt surface and N_2 to the ones in the second layer. This is in agreement with the suggested charge-transfer (CT) direction at the interface of ZnPc and Pt(111).

The N1s binding energy for a ML is 0.60 eV higher than for a ML of ZnPc on Au. This shift is larger than the corresponding C_B and C_P shifts. Another observation is that N1s shifts 0.65 eV to higher binding energy by increasing the coverage from ML to TF, which is larger than observed for C_B (0.33 eV) but close to the value for C_P (0.75 eV). Based on the explanations given earlier for C1s, either nitrogen atoms suffer more from poor core-hole screening in the thick film or the charge transfers at the interface between Pt-C_B and Pt-N are different in the monolayer region.

In order to get a clearer image of the charge transfer between ZnPc and Pt and how the different atoms are affected by this interaction, we present and discuss core-level spectra from the central metal atom. Zn3d spectra are shown in Figure 4(c). The Zn3d peak shows up at 9.46 eV at submonolayer coverage and 9.50 eV for a monolayer, which is at lower BE than ZnPc on Au(111)[5] (9.82 eV). As a result of further ZnPc adsorption, a component at higher BE of the first peak appears in the Zn3d spectrum. At first, by increasing the coverage to 1 ML, the low-BE peak grows but at even higher coverage, the high-BE component becomes dominant and in the molecular thick film only the one at higher BE exists. Thus, we conclude that the low-BE component stems from molecules at the interface, while the high-BE component has contributions from molecules without direct contact with the substrate. The binding-energy shift between these two peaks is 0.6 eV for all preparations in which they coexist. In the thick film, the interfacial component is absent, since there is no or only a very weak contribution from the interface to the photoemission signal of the thick film. A lower binding energy of the interfacial component compared to the molecular-like one is due to the availability of more electrons at the interface. The energy difference between the low-BE peak of ML and the TF peak (1.1 eV) is larger than the energy shift observed for N (0.65 eV), C_P (0.75 eV), and C_B (0.32 eV). This means that the interfacial interaction has the greatest effect on the Zn. The TF peak experiences a shift to a higher BE compared to the high-BE peak of the ML region, implying that Zn, unlike C and N is not decoupled from the substrate at this coverage. Furthermore, the comparison of core-level binding energies on Pt(111) and Au(111) reveals that C1s and N1s have higher binding energies on Pt while for the Zn3d spectra, the binding energy for a ML on Pt is lower than on Au(111). In other words, the inhomogeneous charge distribution is more pronounced when ZnPc is adsorbed on Pt.

The difference in coverage-dependent shifts for different components can be comprehended by several parameters affecting the energy shifts. It can be due to either local or global effects. Since a global effect is expected to influence the shifts for different components almost equally, a more local initial or/and final state effect should be responsible for the diverse BE shifts in this system. One possible explanation is different screening for different atoms. Peisert *et al.* showed

that for ZnPc (and MgPc) adsorbed on Au(100), polarization screening is not enough and contributions from charge-transfer screening have to be considered.[19,68] Charge-transfer screening is more local compared to polarization screening. An inhomogeneous charge transfer for *M*Pc molecules has been reported before.[11,12,19,53] Peisert *et al.* reported different shifts between different atoms when MgPc was adsorbed on Au(111): −0.6 eV for Mg as well as C_P and −0.4 eV for C_B and N. They suggested that this inhomogeneity is a result of different molecule-substrate distances and/or a site-dependent wave function overlap between the metal and the organic molecule.[11] Both these effects influence the charge transfer time scales.

An XSW (X-ray Standing Wave) and ARPES (Angle Resolved Photo Emission Spectroscopy) study of ZnPc on Cu(111) demonstrated site-specific molecule-substrate interactions[53] and showed that ZnPc is distorted on Cu(111), i.e., the Zn atom is pulled down toward the substrate while the organic rings are located farther from the substrate. They observed different thickness-dependent shifts for different atoms due to a change of the molecular geometry and the atom-substrate distances. Interestingly, by fluorination of ZnPc, they observed an increase in the molecular-layer distance to the substrate followed by a decrease in height variations for different atoms of ZnPc (a decrease of the protrusion of Zn) and consequently smaller energy shifts.[53] Thus, based on literature and our own observations, it is very probable that ZnPc is also distorted on Pt. A bending of ZnPc, in a way that the Zn atom is pulled down closer to the Pt surface and the organic rings are bent upwards, together with the fact that Pt donates electrons to ZnPc, would explain the difference in the coverage-dependent shifts as well as the lower BE of Zn3d and the higher BE of C1s and N1s on this surface compared to Au(111). The Zn and C_P atoms experience a different charge transfer than the C_B and N atoms. The details of the different thickness-dependent BE shifts (from our results and references) are given in Table II.

Our results do not provide sufficient evidence that a bending of the molecular plane is the only reason for the site-dependent charge distribution in the molecules. Hence, we also discuss the other possibility, the effect of different wave-function overlap for the different atoms of the molecule with the substrate. Our Pt4f$_{7/2}$ and Zn3d photoemission results confirm Zn-Pt interaction at the interface. Moreover, XAS

TABLE II. Coverage-dependent core-level shifts between a ML and a TF of *M*Pc adsorbed on different substrates. The values are given in units of electronvolts.

	C_B	C_P	N	*M*
ZnPc/TiO$_2$[12]	0.8	1.5	1.7	
FePc/TiO$_2$[47]	1.2	1.1	1.3	…
ZnPc/Au[5]	0.97	0.99	0.70	1.0
FePc/Au[5]	0.40	0.70	0.20	…
ZnPc/Pt	0.32	0.75	0.65	1.1
MgPc/Au[11]	0.40	0.60	0.40	0.60
ZnPc/PtI-$\sqrt{3}$	0.12	0.12	0.08	0.10
ZnPc/PtI-$\sqrt{7}$	0.51	0.48	0.41	0.44

displayed that nitrogen atoms are involved in the interaction between the molecules and the substrate. This is in agreement with the results from the FePc/Ag(111) system, where Fe L-edge and N K-edge XAS confirmed that both Fe and N atoms are involved in the interfacial interaction.[15] Interestingly, the splitting of the first resonance and the change of the line shape were not observed for FePc/Au(100), indicating that N is less involved in the bond to Au than to Ag.[15] Other studies are in line with this; for FePc on Au(111)[5,49] and on Au(110),[1,23] the metal d-states on the central atom are the main molecular contributor to the molecule-surface bond.

Altogether, our core-level-spectroscopy results suggest a non-planar molecular configuration for ZnPc on Pt(111), induced by an attractive Zn-Pt interaction. It is shown that ZnPc molecules do not form a complete monolayer on a Pt surface. Instead, upon increasing the coverage (up to 1 ML), a surface-mediated intermolecular repulsion forces ZnPc into multilayers. The molecules are lying almost parallel to the substrate at lower coverage, while they prefer a tilted position for a higher coverage, due to the decrease of the molecule-substrate interactions. Our photoemission results illustrate that ZnPc is practically decoupled from Pt, starting from the second layer.

B. ZnPc on Pt-I

Adsorption of iodine on Pt(111) leads to two different reconstructions: $(\sqrt{3} \times \sqrt{3})R30°$ at 1/3 ML and $(\sqrt{7} \times \sqrt{7})R19°$ at 3/7 ML iodine coverage.[69] In the case of $(\sqrt{3} \times \sqrt{3})$, iodine occupies threefold hollow sites.[70] For the $(\sqrt{7} \times \sqrt{7})$ reconstruction, both fcc and hcp hollow sites together with the top sites are occupied.[71]

1. Pt4f$_{7/2}$

Pt4f$_{7/2}$ photoemission spectra from the Pt(111)-I surfaces together with their numerical fits are shown in Figure 5. These spectra were measured before and after ZnPc adsorption, as indicated in the figure. The bottom spectrum in Figure 5(a), from $(\sqrt{3} \times \sqrt{3})$ before ZnPc deposition, consists of two peaks: the bulk peak at 70.92 eV and the surface-induced peak at 70.67 eV. The surface shift is 0.25 eV. The relative surface intensity is 42 %. For the $(\sqrt{7} \times \sqrt{7})$ surface the spectrum is practically the same despite the different surface order and different adsorption geometries; the surface shift is 0.24 eV and the relative intensity is 42 %. The top spectra in each panel were recorded after adsorption of ZnPc. There are no observable changes in either of the spectra. The surface shifts and the relative surface intensity remain unaltered. This shows that the ZnPc does not affect Pt when an iodine layer is present.

2. XAS

XAS from ML and TF of ZnPc on Pt-I are presented in Figure 6. They were measured at the same three angles as for the bare Pt substrate above. On $(\sqrt{3} \times \sqrt{3})$ the angular dependence of the $\pi*$ and $\sigma*$ intensities implies a flat lying
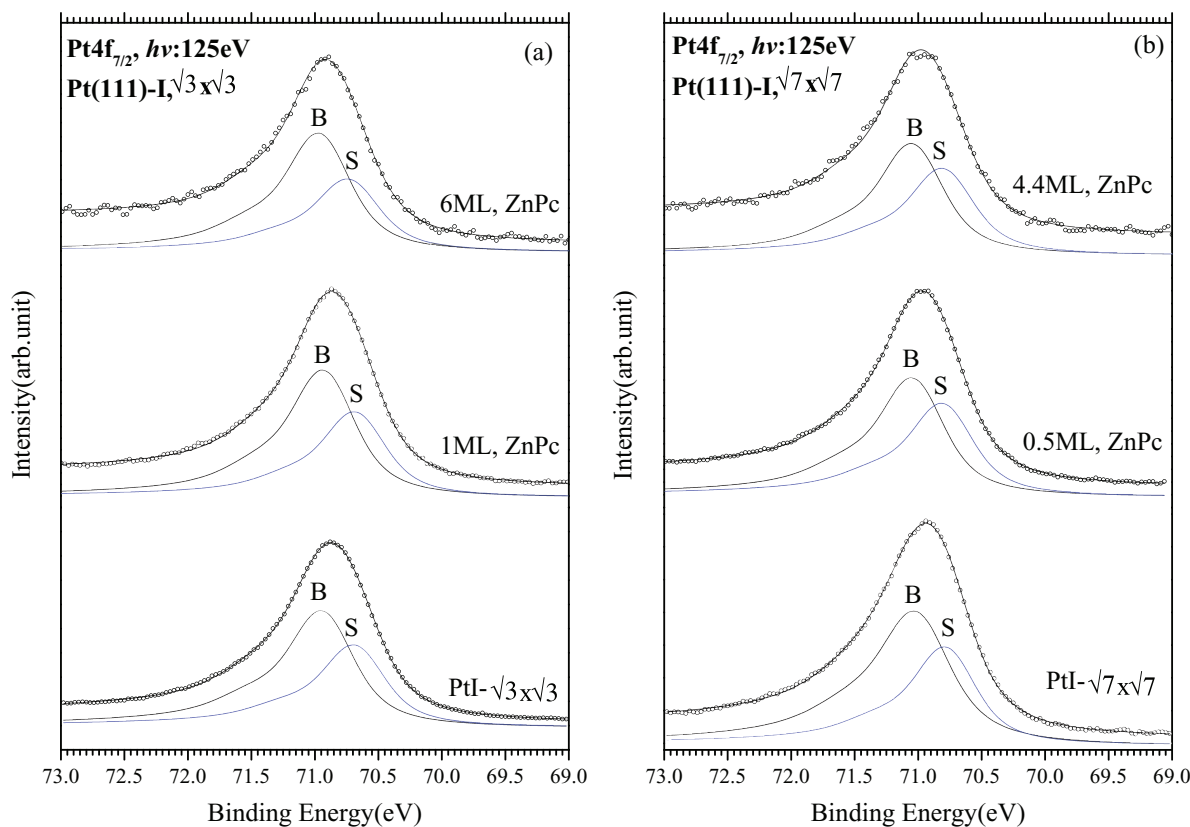

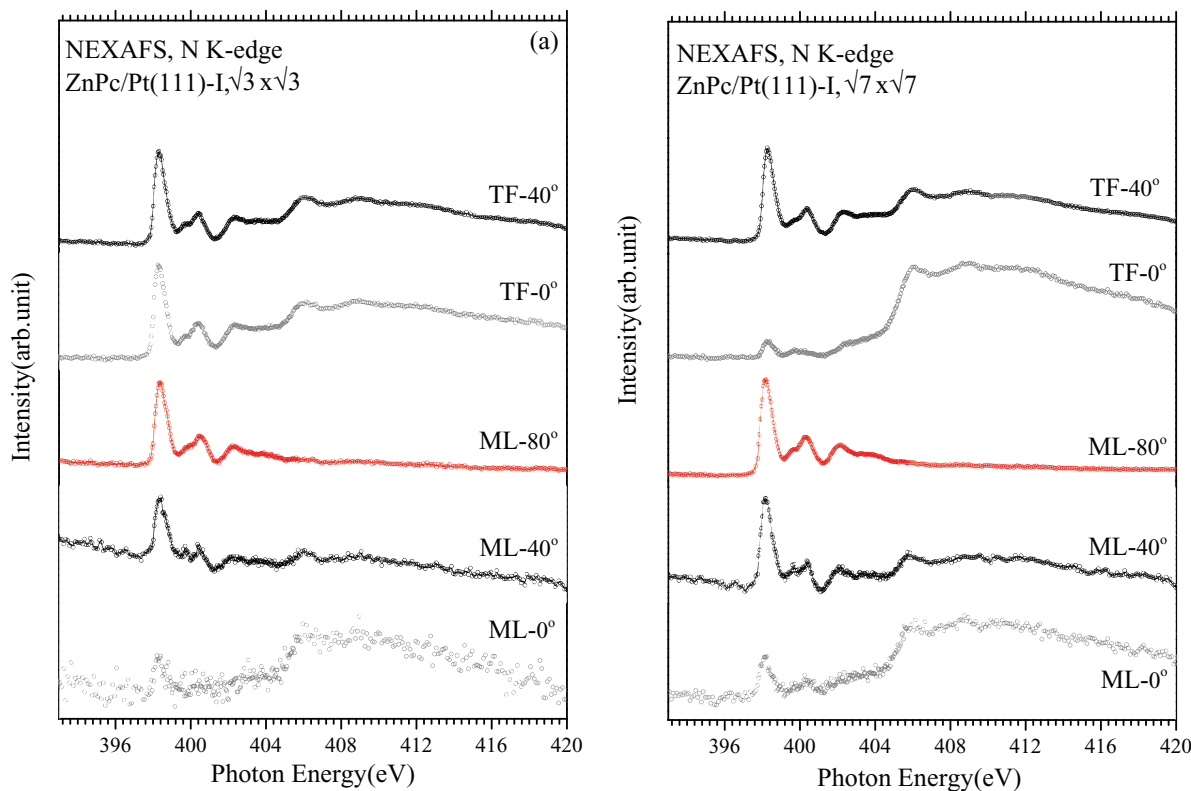FIG. 5. Pt4f spectra of ZnPc on (a) PtI-$(\sqrt{3} \times \sqrt{3})R30°$ and (b) PtI-$(\sqrt{7} \times \sqrt{7})R19°$.

FIG. 6. N K-edge NEXAFS spectra of monolayers and thick films of ZnPc on (a) PtI-$(\sqrt{3} \times \sqrt{3})R30°$ and (b) PtI-$(\sqrt{7} \times \sqrt{7})R19°$.

geometry at ML coverage. At increasing coverage the molecules adopt a slightly tilted geometry. On $(\sqrt{7} \times \sqrt{7})$ the monolayer also appears to lie down flat on the surface and keep this orientation at higher coverage. A closer look at the first resonance reveals that the extra shoulder on the low-photon-energy side observed in Figure 1 is not present here, indicating that N is less involved in the interfacial interactions than on Pt(111).

3. Molecular core levels

Fig. 7(a) shows Zn3d spectra from ZnPc on $(\sqrt{3} \times \sqrt{3})$, where the Zn3d signal appears as a single peak at 10.13 eV. This is 0.65 eV higher than for ZnPc on Pt(111). In addition, there is no observable coverage-dependent shift. Figure 7(b) presents the corresponding Zn3d spectra from ZnPc on $(\sqrt{7} \times \sqrt{7})$. The binding energy at the lowest coverage is lower than on $(\sqrt{3} \times \sqrt{3})$, but higher than on bare Pt. Moreover, the thickness-dependent shift is 0.47 eV here, larger than on $(\sqrt{3} \times \sqrt{3})$ but smaller than on Pt.

C1s measured from increasingly thick ZnPc films on $(\sqrt{3} \times \sqrt{3})$ are shown in Figure 8(a). The same two components (C_B and C_P) obtained for the thick film on the (1×1) surface can be fitted to all spectra. There is practically no coverage-dependent shift. C_B and C_P are located at slightly lower BE than on Pt(111), and they keep their energy separation at all coverages. The N1s spectra are presented in Figure 8(b). Again, and similar to the C1s and Zn3d levels, there is no coverage-dependent shift; the binding energy is stable at 398.15 eV. The low-coverage binding energies of

N1s and C1s are just a little smaller than the low-coverage results from (1×1), whereas for Zn3d the difference is larger.

C1s and N1s spectra from ZnPc on $(\sqrt{7} \times \sqrt{7})$ are presented in Figures 8(c) and 8(d), respectively. At the lowest coverage, the binding energies are lower than for $(\sqrt{3} \times \sqrt{3})$. However, with increasing thickness, both C1s and N1s shift to higher binding energies. The curve fitting reveals the presence of different components in the first layer, B_1, P_1, and N_1 and components from the growing film (B_2, P_2, and N_2). These interface components together with the coverage-dependent shift suggest a charge transfer from the substrate to the molecules. The coverage-dependent shifts are 0.52 eV for benzene carbon, 0.57 eV for pyrrole carbon, and 0.52 eV for nitrogen, thus very close to the Zn3d shift of 0.47 eV.

On Pt(111) a Pt-Zn mediated interaction, including charge transfer and a deformation of the molecular plane, was suggested, based on different thickness dependent shifts. For both iodine substrates, the thickness-dependent shifts are about the same for all atoms, in strong contrast to the findings on Pt(111) (see Table II), indicating a homogeneous charge distribution and charge transfer screening. Interestingly, for $\sqrt{3} \times \sqrt{3}$ there is no coverage dependent shift at all. The origin of the coverage dependent shift is a reduced screening of the core hole when the distance to the surface increases. Obviously, the charge transport time to the core hole depends on the conductivity of the organic film, which apparently is higher on $(\sqrt{3} \times \sqrt{3})$ than on $(\sqrt{7} \times \sqrt{7})$ than on (1×1). The conductivity can have different origins; structure within the film[41] and doping or perhaps a combination.
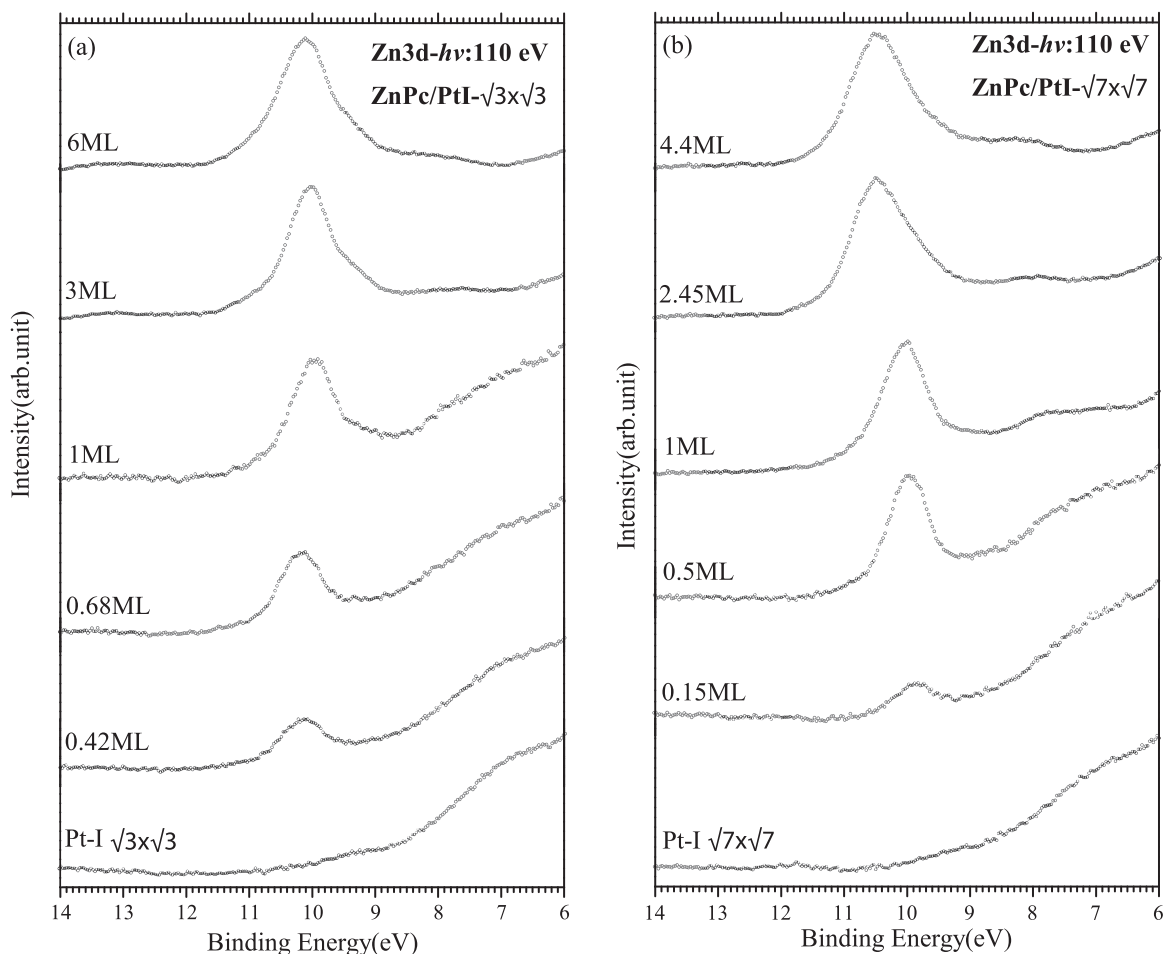
FIG. 7. Zn3d photoemission spectra of ZnPc layers on (a) PtI- $(\sqrt{3} \times \sqrt{3})R30°$ and (b) PtI-$(\sqrt{7} \times \sqrt{7})R19°$.

4. I4d

The I4d spectra, together with their numerical fits are presented in Figure 9. The $(\sqrt{3} \times \sqrt{3})$ spectra are presented in the left panel and from $(\sqrt{7} \times \sqrt{7})$ in the right panel. The amount of deposited ZnPc is indicated in the figure. The $(\sqrt{3} \times \sqrt{3})$ spectrum is fitted with one spin-orbit doublet, I_1 at 51.15 eV ($I4d_{3/2}$), representing hollow site iodine, while the $(\sqrt{7} \times \sqrt{7})$ spectrum holds two clearly separate components (I_1 and I_2) at 50.91 eV and 49.87 eV binding energies. I_1 represents hollow-site iodine and I_2 represents top-site iodine. This shift has been observed previously[69,72] and it was explained as being essentially due to the distance between the iodine adatom and the surface rather than the ionicity/charge on the adatom.[73]

The adsorption of ZnPc induces changes in the I4d spectra from both surfaces. On $(\sqrt{7} \times \sqrt{7})$ I_1 narrows and shifts slightly to higher binding energy. I_2 shifts closer to I_1, i.e., even more to higher binding energy and is also reduced in intensity. On $(\sqrt{3} \times \sqrt{3})$ the I_2 peak develops and at the same time both peaks shift gradually to higher binding energy. At the highest coverage the I4d spectra are rather similar.

The appearance of I_2 on the $\sqrt{3} \times \sqrt{3}$ surface may at first seem surprising, since very small, if any, changes were observed in C1s, N1s, Zn3d, and Pt4f$_{7/2}$ spectra. One further observation is important; the relative intensity of I_2 increases with the ZnPc coverage, thus it is not an interface effect. Instead we suggest that iodine is taken from the Pt surface and dissolved in the ZnPc thin film. Iodine has been used as dopant in organic films for many years.[74–82] Depending on the concentration the conductivity in, for example, PbPc was increased by as much as nine orders of magnitude.[77]

The I_2 from the $\sqrt{3} \times \sqrt{3}$ surface component is shifted to lower binding energy, which in a simple picture signifies a higher local electron density and/or good conductivity for screening of the final state core hole. The screening of the core hole cannot be better than when the iodine is in direct contact with Pt, so we propose that the shift is due to iodine being in a negatively charged state, i.e., it acts as an acceptor dopant in the ZnPc film. This is in agreement with previous results in NiPc[77] and pentacene.[80]

On $(\sqrt{7} \times \sqrt{7})$ there is a coverage dependent shift in C1s, N1s, and Zn3d, which suggest that the iodine doping is lesser in this case. The shifts are smaller than on Pt(111), thus there is most probably doping. The dopant related I_2 component unfortunately overlaps with the original I_2 component, thus iodine doping cannot unambiguously be confirmed by our I4d spectra.

Doping and differences in conductivity will also affect the structure and relative molecular orientation in the organic
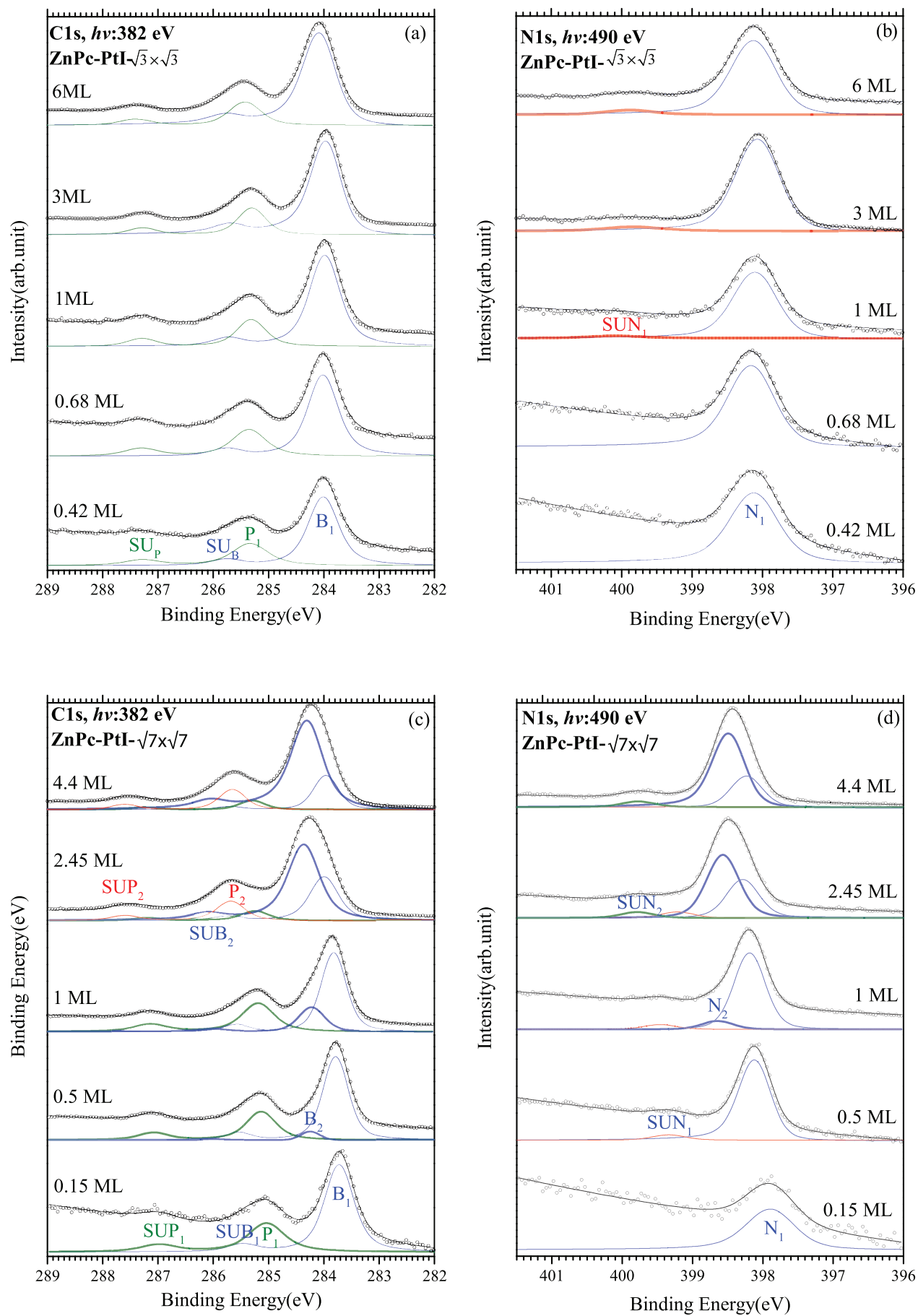
FIG. 8. (a) C1s spectra and (b) N1s spectra from ZnPc on PtI- $(\sqrt{3} \times \sqrt{3})R30°$; (c) C1s spectra and (d) N1s spectra from ZnPc on PtI-$(\sqrt{7} \times \sqrt{7})R19°$.
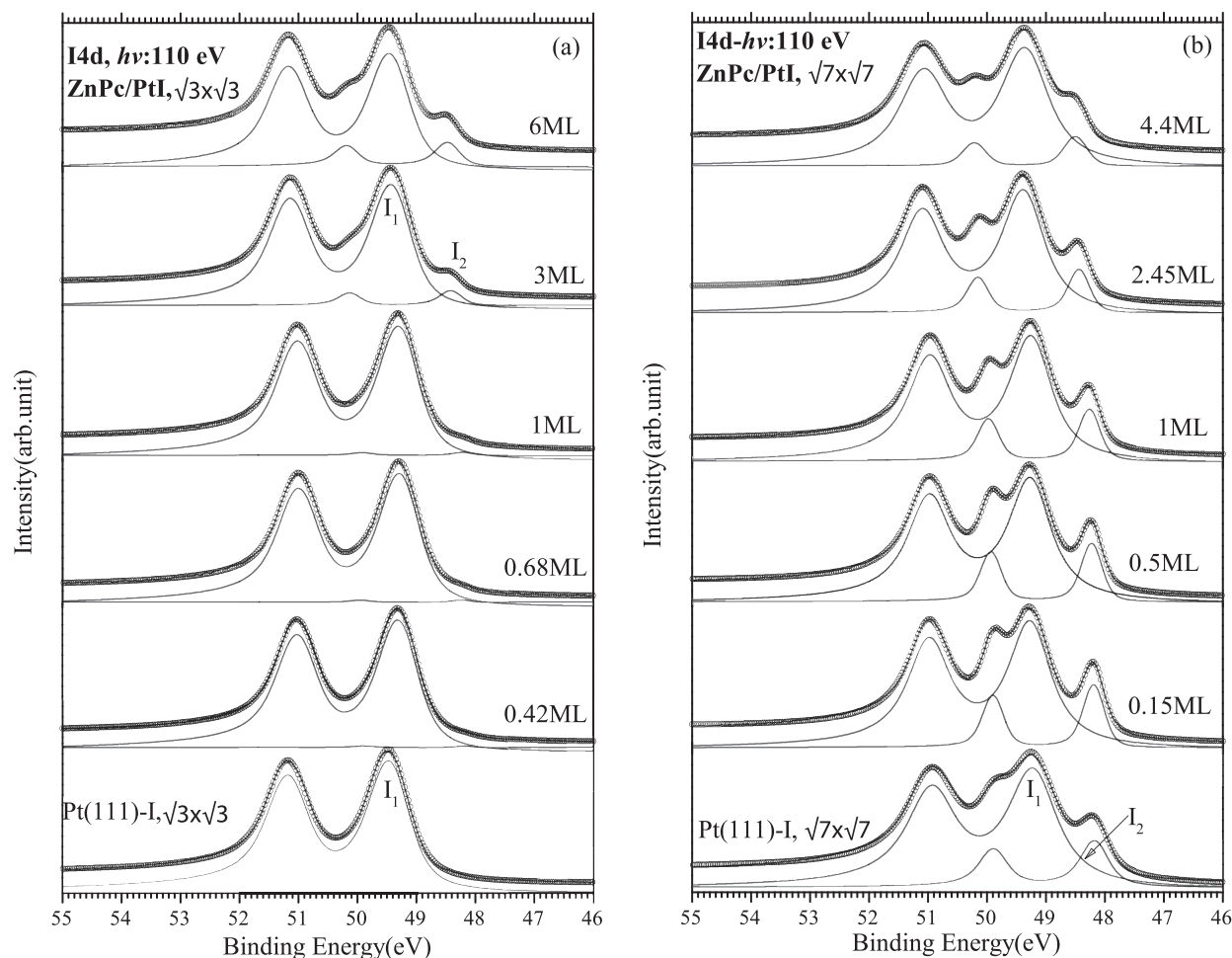
FIG. 9.   I4d spectra from ZnPc on (a) PtI-$(\sqrt{3} \times \sqrt{3})R30°$ and (b) PtI-$(\sqrt{7} \times \sqrt{7})R19°$.

film, since charge distribution within molecules and screening of electrostatic forces will be different.

IV. CONCLUSION

The electronic structure of ZnPc layers, from sub-monolayers to thick films, on Pt(111) is studied by means of X-ray photoelectron spectroscopy (XPS), XAS, and STM. Our core-level-spectroscopy results suggest a non-planar, buckled molecular configuration for ZnPc adsorbed on Pt(111), induced by the Zn-Pt interaction. It is shown that ZnPc molecules do not form a complete monolayer on the Pt surface, due to a surface-mediated intermolecular repulsion. STM images confirm the absence of a well-ordered complete monolayer and depict a porous structure created by ZnPc molecules on Pt(111). Molecules are lying almost parallel to the substrate at lower coverage, while they prefer a tilted position at higher coverage, due to the reduced molecule-substrate interaction. Our photoemission results illustrate that ZnPc is practically decoupled from Pt, starting from the second layer.

Moreover, monolayers of ZnPc have been adsorbed on two different Pt-I reconstructed surfaces; $(\sqrt{3} \times \sqrt{3})R30°$ and $(\sqrt{7} \times \sqrt{7})R19.1°$. Iodine, in particular the $(\sqrt{3} \times \sqrt{3})$ reconstructed surface, reduces the surface-molecule interac-

tion, resulting in a more homogeneous charge distribution and a reduction in the molecular distortion. At increasing ZnPc thickness iodine diffuses from the Pt surface into the molecular film and act as an acceptor creating a hole conducting ZnPc film.

[1]M. G. Betti, P. Gargiani, R. Frisenda, R. Biagi, A. Cossaro, A. Verdini, L. Floreano, and C. Mariani, J. Phys. Chem. C **114**, 21638–21644 (2010).

[2]I. Kröger, B. Stadtmüller, C. Stadler, J. Ziroff, M. Kochler, A. Stahl, F. Pollinger, T.-L. Lee, J. Zegenhagen, F. Reinert, and C. Kumpf, New J. Phys. **12**, 083038 (2010).

[3]K. Nilson, J. Åhlund, M. Shariati, E. Göthelid, P. Palmgren, J. Schiessling, S. Berner, N. Mårtensson, and C. Puglia, J. Phys. Chem. C **114**, 12166–12172 (2010).

[4]J. Åhlund, J. Schnadt, K. Nilson, E. Göthelid, J. Schiessling, F. Besenbacher, N. Mårtensson, and C. Puglia, Surf. Sci. **601**, 3661–3667 (2007).

[5]S. Ahmadi, M. N. Shariati, S. Yu, and M. Göthelid, J. Chem. Phys. **137**, 084705 (2012).

[6] C. Stadler, S. Hansen, I. Kröger, C. Kumpf, and E. Umbach, Nat. Phys. **5**, 153–158 (2009).

[7] C. Stadler, S. Hansen, F. Pollinger, C. Kumpf, E. Umbach, T.-L. Lee, and J. Zegenhagen, Phys. Rev. B **74**, 035404 (2006).

[8] J. D. Baran, J. A. Larsson, R. A. J. Wooley, Y. Cong, P. J. Moriarty, A. A. Cafolla, K. Schulte, and V. R. Dhanak, Phys. Rev. B **81**, 075413 (2010).

[9] M.-S. Liao and S. Scheiner, J. Chem. Phys. **114**, 9780–9791 (2001).

[10] T. Nishi, K. Kanai, Y. Ouchi, M. R. Willis, and K. Seki, in IPAP Conference Series 6, Proceedings of the International Symposium on Super-Functionality Organic Devices (2005) pp. 35–37; pdf available at http://www.ipap.jp/proc/cs6/pdf/cs6_035.pdf.

[11] H. Peisert, A. Petershans, and T. Chassé, J. Phys. Chem. C **112**, 5703–5706 (2008).

[12] S. Yu, S. Ahmadi, C. Sun, P. T. Z. Adibi, W. Chow, A. Pietzsch, and M. Göthelid, J. Chem. Phys. **136**, 154703 (2012).

[13] F. Petraki, H. Peisert, F. Latteyer, U. Aygül, A. Vollmer, and T. Chassé, J. Phys. Chem. C **115**, 21334–21340 (2011).

[14] F. Petraki, H. Peisert, I. Biswas, and T. Chassé, J. Phys. Chem. C **114**, 17638–17643 (2010).

[15] F. Petraki, H. Peisert, U. Aygül, F. Latteyer, J. Uihlein, A. Vollmer, and T. Chassé, J. Phys. Chem. C **116**, 11110–11116 (2012).

[16] F. Petraki, V. Papaefthimiou, and S. Kennou, J. Phys. Conf. Ser. **10**, 135–138 (2005).

[17] J. Xiao and P. A. Dowben, J. Phys.: Condens. Matter **21**, 052001 (2009).

[18] L. Zhang, H. Peisert, I. Biswas, M. Knupfer, D. Batchelor, and T. Chassé, Surf. Sci. **596**, 98–107 (2005).

[19] H. Peisert, D. Kolacyak, and T. Chassé, J. Phys. Chem. C **113**, 19244–19250 (2009).

[20] F. Sedona, M. Di Marino, D. Forrer, A. Vittadini, M. Casarin, A. Cossaro, L. Floreano, A. Verdini, and M. Sambi, Nat. Mater. **11**, 970–977 (2012).

[21] J. Bartolomé, F. Bartolomé, L. M. García, G. Filoti, T. Gredig, C. N. Colesniuc, I. K. Schuller, and J. C. Cezar, Phys. Rev. B **81**, 195405 (2010).

[22] X. Lu, K. Hipps, X. Wang, and U. Mazur, J. Am. Chem. Soc. **118**, 7197–7202 (1996).

[23] P. Gargiani, M. Angelucci, C. Mariani, and M. G. Betti, Phys. Rev. B **81**, 085412 (2010).

[24] S. Riad, Thin Solid Films **370**, 253–257 (2000).

[25] G. de la Torre, C. G. Claessens, and T. Torres, Chem. Commun. **2007**, 2000–2015.

[26] C. G. Claessens, U. Hahn, and T. Torres, Chem. Rec. **8**, 75–97 (2008).

[27] L. S. Hung and C. W. Tang, Appl. Phys. Lett. **74**, 3209–3211 (1999).

[28] G. Gu, G. Parthasarathy, and S. R. Forrest, Appl. Phys. Lett. **74**, 305–307 (1999).

[29] J. Yuan, J. Zhang, J. Wang, X. Yan, D. Yan, and W. Xu, Appl. Phys. Lett. **82**, 3967–3969 (2003).

[30] T. S. Ellis, K. T. Park, S. L. Hulbert, M. D. Ulrich, and J. E. Rowe, J. Appl. Phys. **95**, 982–988 (2004).

[31] Y. Naitoh, T. Matsumoto, K. Sugiura, Y. Sakata, and T. Kawai, Surf. Sci. **487**, L534–L540 (2001).

[32] M. Takada and H. Tada, Jpn. J. Appl. Phys. **44**, 5332–5335 (2005).

[33] I. Biswas, H. Peisert, M. Nagel, M. B. Casu, S. Schuppler, P. Nagel, E. Pellegrin, and T. Chassé, J. Chem. Phys. **126**, 174704 (2007).

[34] Z. H. Cheng, L. Gao, Z. T. Deng, Q. Liu, N. Jiang, X. Lin, X. B. He, S. X. Du, and H. J. Gao, J. Phys. Chem. C **111**, 2656–2660 (2007).

[35] I. Chizhov, G. Scoles, and A. Kahn, Langmuir **16**, 4358–4361 (2000).

[36] A. Cossaro, D. Cvetko, G. Bavdek, L. Floreano, R. Gotter, A. Morgante, F. Evangelista, and A. Ruocco, J. Phys. Chem. B **108**, 14671–14676 (2004).

[37] F. Evangelista, A. Ruocco, V. Corradini, M. P. Donzello, C. Mariani, and M. G. Betti, Surf. Sci. **531**, 123–130 (2003).

[38] Y.-S. Fu, S.-H. Ji, X. Chen, X.-C. Ma, R. Wu, C.-C. Wang, W.-H. Duan, X.-H. Qiu, B. Sun, P. Zhang, J.-F. Jia, and Q.-K. Xue, Phys. Rev. Lett. **99**, 256601 (2007).

[39] L. Gao, W. Ji, Y. B. Hu, Z. H. Cheng, Z. T. Deng, Q. Liu, N. Jiang, X. Lin, W. Guo, S. X. Du, W. A. Hofer, X. C. Xie, and H. Gao, Phys. Rev. Lett. **99**, 106402 (2007).

[40] L. Grządziel, M. Krzywiecki, H. Peisert, T. Chassé, and J. Szuber, Thin Solid Films **519**, 2187–2192 (2011).

[41] S. Yu, S. Ahmadi, C. Sun, K. Schulte, A. Pietzsch, F. Hennies, M. Zuleta, and M. Göthelid, J. Phys. Chem. C **115**, 14969–14977 (2011).

[42] B. Brena, P. Palmgren, K. Nilson, S. Yu, F. Hennies, B. Agnarsson, A. Önsten, M. Månsson, and M. Göthelid, Surf. Sci. **603**, 3160–3169 (2009).

[43] S. Dick, H. Peisert, D. Dini, M. Hanack, M. J. Cook, I. Chambrier, and T. Chassé, J. Appl. Phys. **97**, 073715 (2005).

[44] F. Evangelista, R. Gotter, N. Mahne, S. Nannarone, A. Ruocco, and P. Rudolf, J. Phys. Chem. C **112**, 6509–6514 (2008).

[45] A. Gerlach, F. Schreiber, S. Sellner, H. Dosch, I. A. Vartanyants, B. C. C. Cowie, T.-L. Lee, and J. Zegenhagen, Phys. Rev. B **71**, 205425 (2005).

[46] S. Yu, S. Ahmadi, P. Palmgren, F. Hennies, M. Zuleta, and M. Göthelid, J. Phys. Chem. C **113**, 13765–13771 (2009).

[47] P. Palmgren, S. Yu, F. Hennies, K. Nilson, B. Åkermark, and M. Göthelid, J. Chem. Phys. **129**, 074707 (2008).

[48] C. Isvoranu, B. Wang, K. Schulte, E. Ataman, J. Knudsen, J. N. Andersen, M. L. Bocquet, and J. Schnadt, J. Phys. Condens. Matter **22**, 472002 (2010).

[49] C. Isvoranu, B. Wang, E. Ataman, K. Schulte, J. Knudsen, J. N. Andersen, M. Bocquet, and J. Schnadt, J. Chem. Phys. **134**, 114710 (2011).

[50] C. Isvoranu, B. Wang, E. Ataman, K. Schulte, J. Knudsen, J. N. Andersen, M.-L. Bocquet, and J. Schnadt, J. Phys. Chem. C **115**, 20201–20208 (2011).

[51] C. Isvoranu, B. Wang, E. Ataman, J. Knudsen, K. Schulte, J. N. Andersen, M.-L. Bocquet, and J. Schnadt, J. Phys. Chem. C **115**, 24718–24727 (2011).

[52] C. Isvoranu, J. Knudsen, E. Ataman, K. Schulte, B. Wang, M.-L. Bocquet, J. N. Andersen, and J. Schnadt, J. Chem. Phys. **134**, 114711 (2011).

[53] H. Yamane, A. Gerlach, S. Duhm, Y. Tanaka, T. Hosokai, Y. Y. Mi, J. Zegenhagen, N. Koch, K. Seki, and F. Schreiber, Phys. Rev. Lett. **105**, 046103 (2010)

[54] R. Nyholm, S. Svensson, J. Nordgren, and A. Flodström, Nucl. Instrum. Methods Phys. Res., Sect. A **246**, 267–271 (1986).

[55] S. Doniach and M. Šunjić, J. Phys. C: Solid State Phys. **3**, 285–291 (1970).

[56] C. Puglia, A. Nilsson, B. Hernnäs, O. Karis, P. Bennich, and N. Mårtensson, Surf. Sci. **342**, 119–133 (1995).

[57] E. Janin, S. Ringler, J. Weissenrieder, T. Åkermark, U. O. Karlsson, M. Göthelid, D. Nordlund, and H. Ogasawara, Surf. Sci. **482–485**, 83–89 (2001).

[58] J. F. Zhu, M. Kinne, T. Fuhrmann, R. Denecke, and H.-P. Steinrück, Surf. Sci **529**, 384–396 (2003).

[59] O. Björneholm, A. Nilsson, H. Tillborg, P. Bennich, A. Sandell, B. Hernnäs, C. Puglia, and N. Mårtensson, Surf. Sci **315**, L983–L989 (1994).

[60] Z. H. Cheng, L. Gao, Z. T. Deng, N. Jiang, Q. Liu, D. X. Shi, S. X. Du, H. M. Guo, and H.-J. Gao, J. Phys. Chem. C **111**, 9240–9244 (2007).

[61] L. Zhang, Z. Cheng, Q. Huan, X. He, X. Lin, L. Gao, Z. Deng, N. Jiang, Q. Liu, S. Du, H. Guo, and H. Gao, J. Phys. Chem. C **115**, 10791–10796 (2011).

[62] M.-N. Shariati, J. Lüder, I. Bidermane, S. Ahmadi, E. Göthelid, P. Palmgren, B. Sanyal, O. Eriksson, M. N. Piancastelli, B. Brena, and C. Puglia, J. Phys. Chem. C **117**, 7018–7025 (2013).

[63] F. Evangelista, A. Ruocco, R. Gotter, A. Cossaro, L. Floreano, A. Morgante, F. Crispoldi, M. G. Betti, and C. Mariani, J. Chem. Phys. **131**, 174710 (2009).

[64] H. Peisert, M. Knupfer, T. Schwieger, J. M. Auerhammer, M. S. Golden, and J. Fink, J. Appl. Phys. **91**, 4872–4878 (2002).

[65] T.-W. Pi, G.-R. Lee, C.-H. Wei, W.-Y. Chen, and C.-P. Cheng, J. Appl. Phys. **106**, 113716 (2009).

[66] A. Ruocco, F. Evangelista, R. Gotter, A. Attili, and G. Stefani, J. Phys. Chem. C **112**, 2016–2025 (2008).

[67] J. Åhlund, K. Nilson, J. Schiessling, L. Kjeldgaard, S. Berner, N. Mårtensson, C. Puglia, B. Brena, M. Nyberg, and Y. Luo, J. Chem. Phys. **125**, 034709 (2006).

[68] D. Kolacyak, H. Peisert, and T. Chassé, Appl. Phys. A **95**, 173–178 (2009).

[69] S. B. DiCenzo, G. K. Wertheim, and D. N. E. Buchanan, Phys. Rev. B **30**, 553–557 (1984).

[70] A. Tkatchenko, N. Batina, A. Cedillo, and M. Galván, Surf. Sci. **581**, 58–65 (2005).

[71] S. K. Jo and J. M. White, Surf. Sci. **261**, 111–117 (1992).

[72] M. Göthelid, M. Tymczenko, W. Chow, S. Ahmadi, S. Yu, B. Bruhn, D. Stoltz, H. von Schenck, J. Weissenrieder, and C. Sun, J. Chem. Phys. **137**, 204703 (2012).

[73] P. S. Bagus, C. Wöll, and A. Wieckowski, Surf. Sci. **603**, 273–283 (2009).

[74] J. Curry and E. P. Cassidy, J. Chem. Phys. **37**, 2154–2155 (1962).

[75]W. A. Orr and S. C. Dahlberg, J. Am. Chem. Soc. **101**, 2875–2880 (1979).

[76]C. J. Schramm, R. P. Scaringe, D. R. Stojakovic, B. M. Hoffman, J. A. Ibers, and T. J. Marks, J. Am. Chem. Soc. **102**, 6702–6713 (1980).

[77]W. Wacławek and M. Ząbkowska-Wacławek, Thin Solid Films **146**, 1–6 (1987).

[78]S. Nakamura, H. Amatatsu, T. Ozaki, S. Yamaguchi, and G. Sawa, Jpn. J. Appl. Phys. **26**, 1878–1883 (1987).

[79]G. D. Sharma, S. G. Sangodkar, and M. S. Roy, Mater. Sci. Eng., B **41**, 222–227 (1996).

[80]M. Brinkmann, V. S. Videva, A. Bieber, J. J. André, P. Turek, L. Zuppiroli, P. Bugnon, M. Schaer, F. Nuesch, and R. Humphry-Baker, J. Phys. Chem. A **108**, 8170–8179 (2004).

[81]K. Hayashi, T. Shinano, Y. Miyazaki, and T. Kajitani, J. Appl. Phys. **109**, 023712 (2011).

[82]S. Mizuta, M. Iyota, S. Tanaka, and I. Hiromitsu, Thin Solid Films **520**, 5761–5769 (2012).